

# A Domain Decomposition Inspired 2D Nodal Integration method for Helmholtz Problems Leading to Well Conditioned Matrix Problems

Martin J. Gander<sup>[0000-0001-8450-9223]</sup>,  
Niteen Kumar<sup>[0000-0003-0960-0136]</sup>

## 1 Introduction

The Helmholtz equation is one of the fundamental partial differential equations (PDEs) which found its application in a variety of domains. It is used to describe pressure fields in acoustics, electromagnetic fields in space, modes of resonance in structural dynamics, and neutron dynamics in reactors. Many numerical schemes have been developed, but most of the legacy codes are based on schemes like finite difference methods (FDMs), finite element methods (FEMs), discontinuous Galerkin (DG) methods or finite volume methods (FVMs), which require fine mesh or complex nodal dependency for desired levels of accuracy [4, 9]. The resulting matrix system with these methods are very large and badly conditioned, and make it inefficient to use iterative solvers for large wave numbers, see e.g. [2, 3, 6] and references therein. It is also well established that Helmholtz problems pose significant challenges when solved using iterative methods [10]. To address these issues, we present here a 2D Nodal Integration Method (NIM) based on domain decomposition for the Helmholtz equation,

$$\Delta u(x, y) + k^2 u(x, y) = f(x, y), \quad (1)$$

where  $(x, y)$  is the spatial position,  $k$  is the wave number,  $u$  represents the wave field, typically a pressure distribution, and  $f$  is the source term. NIM is a semi-analytical coarse mesh numerical scheme. NIM was originally developed for the solution of neutron diffusion equations to find the distribution of neutrons in a nuclear reactor, and due to its high accuracy with coarse meshes, NIM found its acceptance in other engineering domains as well, see e.g. [5] and references therein. In NIM, first the

---

Martin J. Gander

Section de mathématiques, Université de Genève, Rue du Conseil-Général 9, CP 64, 1211 Genève 4, Switzerland, e-mail: martin.gander@unige.ch

Niteen Kumar

MOX Laboratory, Dipartimento di Matematica, Politecnico di Milano, Piazza Leonardo da Vinci 32, 20133 Milano, Italy, e-mail: niteenkumar@polimi.it

PDE is averaged in one direction by merging all other directional derivatives into the source, which is called pseudo source. These pseudo sources are then expanded using Legendre polynomials and the order of the scheme is dependent on the number of terms kept in the expansion. For example, expanding up to constant terms results in a second order scheme. This expansion gives us a set of ordinary differential equations (ODEs) with constant source and makes the analytical solution of the resulting ODEs possible [5]. The ODEs are solved analytically within cells called nodes. After the integration, neighboring analytical solutions are connected using coupling conditions. Classically, Dirichlet continuity is imposed by imposing a common (unknown) value, which is then determined imposing Neumann continuity, like in a sub-structuring domain decomposition method. This results in two three-point schemes, one in the  $x$ -direction and the other in the  $y$ -direction. From these three-point schemes, the pseudo source is finally eliminated using constraint conditions, which results in the final set of algebraic equations for the scheme, see [7] for more details. This analytical pre-processing in NIM provides a distinct advantage over other numerical schemes and makes the scheme closer to the underlying physics of the problem, in contrast to basis-function-driven approaches such as the finite element method. NIM schemes are closely related to Trefftz methods [11], introduced by Erich Trefftz in 1926. Trefftz methods use basis functions that exactly satisfy the homogeneous equations within each element (see [3] and references therein), whereas NIMs satisfy only one-dimensional averaged equations. We refer to [7] for the details of the derivation of such a classical NIM scheme for the two dimensional Helmholtz equation, and present the resulting system of algebraic equations and their coefficients in the Appendix. Discretization in numerical schemes inherently introduces dispersion errors. Due to their analytical pre-processing, NIM schemes exhibit significantly lower dispersion than conventional methods (see [7, 13], and references therein for details on dispersion correction). Although the original NIM scheme for the Helmholtz equation is functional, its matrix elements exhibit a strong dependence on the wave number  $k$  and for some values of  $k$  face division by zero. To address this issue, we design here a new Helmholtz NIM that avoids in its construction the solution of Helmholtz problems with Dirichlet conditions that can become ill-posed. This can be achieved by using impedance conditions instead, like it was proposed in the seminal work of Després and his non-overlapping Schwarz method for Helmholtz problems [8].

We propose here a new NIM scheme for the Helmholtz equation in 2D to improve the conditioning of the resulting system matrix, and further reduce dispersion. This study extends our previous work conducted in one dimension [1]. Our new approach uses impedance (or Robin) conditions in its construction, in contrast to the classical Dirichlet and Neumann conditions in earlier NIMs for Helmholtz problems. Instead of the unknown Dirichlet values  $u_j$  in the original Helmholtz NIM, now the unknowns are impedance traces, which means that we construct directly a right preconditioned system in this new Helmholtz NIM design.

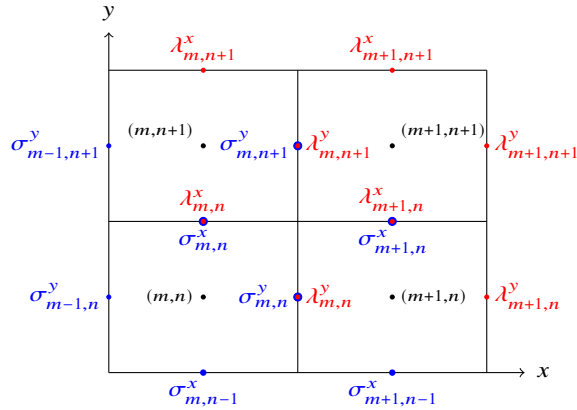


**Fig. 1** Arrangement of 4 nodes in 2D,  $\sigma^x$ ,  $\sigma^y$ ,  $\lambda^x$  and  $\lambda^y$  are traces of impedance conditions at the node interfaces.

### 2 NIM scheme using impedance transmission conditions

In order to derive the NIM scheme for the 2D Helmholtz equation given in (1), the domain is divided into  $(n \times n)$  square elements of size  $(h \times h)$  called nodes, shown in Figure 1. For each node, a local coordinate system is defined with origin at the node center. Equation (1) can be written with reference to node  $(m, n)$  as

$$\Delta u_{m,n}(x, y) + k^2 u_{m,n}(x, y) = f_{m,n}(x, y), \quad (x, y) \in \left(-\frac{h}{2}, \frac{h}{2}\right) \times \left(-\frac{h}{2}, \frac{h}{2}\right). \quad (2)$$

First the PDE is averaged within the node to remove the dependency in one spatial direction, which results in a transverse averaged ODE. This is called the transverse integration process (TIP). It is performed by averaging (2) with the operator  $\frac{1}{h} \int_{-h/2}^{+h/2} dx$  in the  $x$ -direction, resulting in a  $y$ -dependent ODE,

$$\frac{1}{h} \int_{-h/2}^{+h/2} \left( \frac{\partial^2 u_{m,n}(x, y)}{\partial x^2} + \frac{\partial^2 u_{m,n}(x, y)}{\partial y^2} + k^2 u_{m,n}(x, y) = f_{m,n}(x, y) \right) dx, \quad (3)$$

$$\implies \frac{d^2 \bar{u}_{m,n}^x(y)}{dy^2} + k^2 \bar{u}_{m,n}^x(y) = \bar{S}_{m,n}^x(y). \quad (4)$$

Similarly, the operator  $\frac{1}{h} \int_{-h/2}^{+h/2} dy$  is used for averaging in the  $y$ -direction, resulting in an  $x$ -dependent ODE,

$$\frac{1}{h} \int_{-h/2}^{+h/2} \left( \frac{\partial^2 u_{m,n}(x, y)}{\partial x^2} + \frac{\partial^2 u_{m,n}(x, y)}{\partial y^2} + k^2 u_{m,n}(x, y) = f_{m,n}(x, y) \right) dy, \quad (5)$$

$$\implies \frac{d^2 \bar{u}_{m,n}^y(x)}{dx^2} + k^2 \bar{u}_{m,n}^y(x) = \bar{S}_{m,n}^y(x). \quad (6)$$

Here, the variables  $\bar{u}_{m,n}^x$  and  $\bar{u}_{m,n}^y$  represent averaged quantities,

$$\bar{u}_{m,n}^x(y) := \frac{1}{h} \int_{-h/2}^{+h/2} u_{m,n}(x,y) dx, \quad \bar{u}_{m,n}^y(x) := \frac{1}{h} \int_{-h/2}^{+h/2} u_{m,n}(x,y) dy,$$

and the source term  $f_{m,n}$  is averaged along with the remaining transverse term as,

$$\bar{S}_{m,n}^x(y) = \frac{1}{h} \int_{-h/2}^{+h/2} \left( f_{m,n} - \frac{\partial^2 u_{m,n}}{\partial x^2} \right) dx, \quad \bar{S}_{m,n}^y(x) = \frac{1}{h} \int_{-h/2}^{+h/2} \left( f_{m,n} - \frac{\partial^2 u_{m,n}}{\partial y^2} \right) dy,$$

which we call pseudo source terms. Next, we expand the pseudo source in Legendre polynomials and truncated at zeroth order which results in a second order accurate scheme [5]. Next, the ODE given in (4) is solved analytically over the node  $(m, n)$  with impedance conditions,

$$\left[ -\frac{\partial \bar{u}_{m,n}^{ax}}{\partial y} + ik \bar{u}_{m,n}^{ax} \right]_{-h/2} = \bar{\sigma}_{m,n-1}^x; \quad \left[ \frac{\partial \bar{u}_{m,n}^{ax}}{\partial y} + ik \bar{u}_{m,n}^{ax} \right]_{h/2} = \bar{\lambda}_{m,n}^x, \quad (7)$$

which gives us an analytical expression for  $\bar{u}_{m,n}^{xa}$ ,

$$\bar{u}_{m,n}^{xa}(y) = \frac{2\bar{S}_{m,n}^x + e^{-\frac{ik(h+2y)}{2}} (-\bar{S}_{m,n}^x - e^{2iky} (\bar{S}_{m,n}^x + ik\bar{\lambda}_{m,n}^x) - ik\bar{\sigma}_{m,n-1}^x)}{2k^2}. \quad (8)$$

The same process is repeated for node  $(m, n+1)$  using impedance conditions, and gives us an analytical expression for  $\bar{u}_{m,n+1}^{xa}$ ,

$$\bar{u}_{m,n+1}^{xa}(y) = \frac{2\bar{S}_{m,n+1}^x + e^{-\frac{ik(h+2y)}{2}} (-\bar{S}_{m,n+1}^x - e^{2iky} (\bar{S}_{m,n+1}^x + ik\bar{\lambda}_{m,n+1}^x) - ik\bar{\sigma}_{m,n}^x)}{2k^2}. \quad (9)$$

Similar steps are repeated in the  $x$ -direction, to get analytical expressions of  $\bar{u}_{m,n}^{ya}$  for node  $(m, n)$  and  $\bar{u}_{m+1,n}^{ya}(x)$  for node  $(m+1, n)$ ,

$$\bar{u}_{m,n}^{ya}(x) = \frac{2\bar{S}_{m,n}^y + e^{-\frac{ik(h+2x)}{2}} (-\bar{S}_{m,n}^y - e^{2ikx} (\bar{S}_{m,n}^y + ik\bar{\lambda}_{m,n}^y) - ik\bar{\sigma}_{m-1,n}^y)}{2k^2}, \quad (10)$$

$$\bar{u}_{m+1,n}^{ya}(x) = \frac{2\bar{S}_{m+1,n}^y + e^{-\frac{ik(h+2x)}{2}} (-\bar{S}_{m+1,n}^y - e^{2ikx} (\bar{S}_{m+1,n}^y + ik\bar{\lambda}_{m+1,n}^y) - ik\bar{\sigma}_{m,n}^y)}{2k^2}. \quad (11)$$

Here,  $u^{xa}$  is the analytical solution for the  $x$ -averaged ODEs and  $u^{ya}$  is the analytical solution for the  $y$ -averaged ODEs. Now in order to connect the consecutive nodes in the  $x$ -direction, impedance matching condition are imposed at the interface. This leads to a finite difference like stencil for the unknown  $\bar{\lambda}_{m,n}^x$ , which contains in its coefficients information about the physical problem that is solved,

$$\bar{\sigma}_{m,n+1}^x = \left( ik \bar{u}_{m,n}^{xa}(y) - \frac{d\bar{u}_{m,n}^{xa}(y)}{dy} \right)_{h/2}, \quad \bar{\lambda}_{m,n+1}^x = \left( ik \bar{u}_{m,n+1}^{xa}(y) - \frac{d\bar{u}_{m,n+1}^{xa}(y)}{dy} \right)_{-h/2}. \quad (12)$$

This leads to

$$-\frac{\iota \bar{S}_{m,n}^x}{k} + \frac{\iota e^{-\iota hk} \bar{S}_{m,n}^x}{k} + \bar{\sigma}_{m,n}^x - e^{-\iota hk} \bar{\sigma}_{m,n-1}^x = 0, \quad (13)$$

$$-\frac{\iota \bar{S}_{m,n+1}^x}{k} + \frac{\iota e^{-\iota hk} \bar{S}_{m,n+1}^x}{k} + \bar{\lambda}_{m,n}^x - e^{-\iota hk} \bar{\lambda}_{m,n+1}^x = 0. \quad (14)$$

Similarly, to get the node stencil in the  $y$ -direction, an impedance matching condition is imposed at the interface, which leads to

$$-\frac{\iota \bar{S}_{m,n}^y}{k} + \frac{\iota e^{-\iota hk} \bar{S}_{m,n}^y}{k} + \bar{\sigma}_{m,n}^y - e^{-\iota hk} \bar{\sigma}_{m-1,n}^y = 0, \quad (15)$$

$$-\frac{\iota \bar{S}_{m+1,n}^y}{k} + \frac{\iota e^{-\iota hk} \bar{S}_{m+1,n}^y}{k} + \bar{\lambda}_{m,n}^y - e^{-\iota hk} \bar{\lambda}_{m+1,n}^y = 0. \quad (16)$$

Next, we need to eliminate the pseudo source terms from (13), (14), (15) and (16). For this, we use constraint conditions,

$$\bar{u}_{m,n}^{xy} = \bar{u}_{m,n}^{yx}; \quad \bar{S}_{m,n}^x + \bar{S}_{m,n}^y - \frac{1}{h} \int_{-h/2}^{+h/2} \left( \frac{1}{h} \int_{-h/2}^{+h/2} u_{m,n}(x,y) dy \right) dx = S_{m,n}. \quad (17)$$

The pseudo source terms are obtained by solving (17), and putting the pseudo source back into (13), (14), (15) and (16) we get the final form of the NIM equations,

$$\lambda_{m,n}^y + D\lambda_{m+1,n}^y + B(\lambda_{m+1,n}^x + \sigma_{m+1,n-1}^x) + A\sigma_{m,n}^y + ES_{m+1,n} = 0, \quad (18)$$

$$A\lambda_{m,n}^y + B(\lambda_{m,n}^x + \sigma_{m,n-1}^x) + \sigma_{m,n}^y + D\sigma_{m-1,n}^y + ES_{m,n} = 0, \quad (19)$$

$$\lambda_{m,n}^x + D\lambda_{m,n+1}^x + A\sigma_{m,n}^x + B(\lambda_{m,n+1}^y + \sigma_{m-1,n+1}^y) + ES_{m,n+1} = 0, \quad (20)$$

$$A\lambda_{m,n}^x + \sigma_{m,n}^x + D\sigma_{m,n-1}^x + B(\lambda_{m,n}^y + \sigma_{m-1,n}^y) + ES_{m,n} = 0, \quad (21)$$

with the coefficients  $A, B, D, E$  given in the Appendix. A Taylor expansion of the scheme for  $h \rightarrow 0$  shows first-order convergence.

To complete the linear system, we need to derive expressions for the boundary nodes as well. We assume the boundary condition to be of impedance type. To derive the expression for the left and right, the original impedance boundary condition is applied to  $\bar{u}_{m,n}^{ya}$  from (10) and for the top and bottom, the impedance boundary condition is applied to  $\bar{u}_{m,n}^{xa}$  from (8). This gives us four equations, and completes the matrix system (L, R, T, and B denote the left, right, top, and bottom boundaries),

$$\left[ -\frac{\partial \bar{u}_{m,n}^{ya}}{\partial x} + \iota k \bar{u}_{m,n}^{ya} \right]_{(-\frac{h}{2}) \rightarrow (L,B)} = 0, \quad \left[ \frac{\partial \bar{u}_{m,n}^{xa}}{\partial y} + \iota k \bar{u}_{m,n}^{xa} \right]_{(\frac{h}{2}) \rightarrow (R,T)} = 0. \quad (22)$$

To recover the original solution  $u$  from the Robin traces  $\sigma, \lambda$ , we take the average of the two traces, i.e.,  $u = (\sigma + \lambda)/(2\iota k)$ .

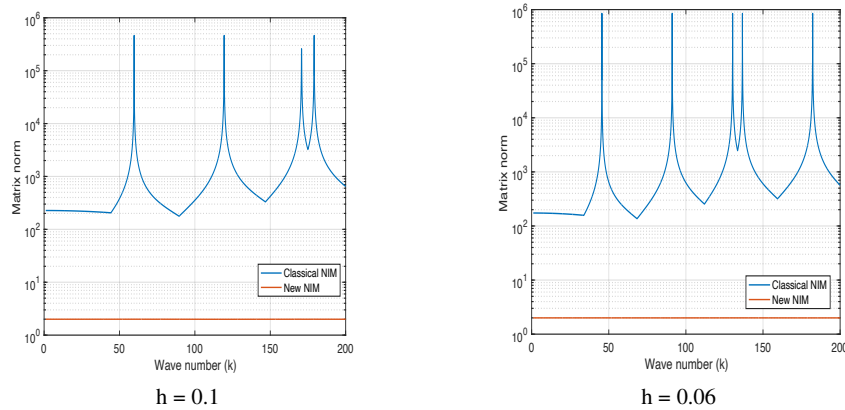


**Fig. 2** Comparison of the matrix norms between the classical NIM and the new NIM for a range of wave numbers  $k = (1 : 200)$ , with two mesh sizes ( $h = 0.1, 0.06$ )

### 3 Numerical Experiments

We use a classical wave field problem with impedance boundary conditions to demonstrate the properties of the new NIM method developed here. We show in Figure 2 the  $l_2$  norms of the classical and new NIM for two different mesh sizes and many values of the wave number  $k$ . We see that for the new NIM, the matrix norms stay nicely bounded below 2, whereas for the classical NIM the matrix norms are of the order of  $10^5$ . The presence of the multiple poles in the plots indicates that the matrix norm is extremely sensitive to the wave number  $k$  in the classical NIM, and this does not improve when the mesh is refined. This strong dependence is numerically not desirable, especially when the mesh resolution is not changed as in our example, there is too much sensitivity with respect to the wave number in this discrete problem. We can see the reason for this also looking at the stencil entries in the appendix: in the interior stencil, the stencil coefficients contain a division by  $\cot(kh)$ , and this quantity becomes zero for  $k = \pi(2n + 1)/2h$ ,  $n = 1, 2, \dots$ , which explains the poles in Figure 2, and more generally the sensitivity of the classical Helmholtz NIM matrix norm on the wave number. We can now also explain the reason for this sensitivity: in the construction of the classical Helmholtz NIM, we solved 2D Helmholtz problems on each node, imposing Dirichlet boundary conditions, and if  $k^2$  corresponds to an eigenvalue of the two dimensional Laplacian, then this problem is not well posed, a fact that manifests itself in the division by zero in the stencil coefficients.

## 4 Conclusions

We presented a new 2D nodal integration method (NIM) based on domain decomposition techniques for the Helmholtz equation. In our new Helmholtz NIM, instead of Dirichlet and Neumann transmission conditions that are usually used in the construction of the NIM, we used impedance transmission conditions. This modification changes the coefficients as well as the resulting system matrix structure, and we observe that the new system matrix has nicely bounded norms for all wave numbers, while the original NIM system matrix norm presents singularities. However, the new system matrix is now twice the size of the old system matrix, since we are solving for the Robin traces as unknowns. We gain stability at the cost of a bigger system matrix. We are currently developing our new Helmholtz NIM in three spatial dimensions, and also investigate if it is possible to use impedance conditions without increasing the system matrix size. We are also studying the dispersion relation properties of our new Helmholtz NIM, and investigate its potential for dispersion correction.

## Appendix

If we do not merge  $k^2 u(x, y)$  into the pseudo source, the classical NIM scheme from [7] is given by

$$E(S_{m,n} + S_{m,n+1}) + H(\bar{u}_{m,n}^y + \bar{u}_{m,n+1}^y + \bar{u}_{m-1,n}^y + \bar{u}_{m-1,n+1}^y) + F\bar{u}_{m,n}^x + G(\bar{u}_{m,n-1}^x + \bar{u}_{m,n+1}^x) = 0,$$

$$E(S_{m,n} + S_{m+1,n}) + D(\bar{u}_{m,n}^x + \bar{u}_{m,n-1}^x + \bar{u}_{m+1,n}^x + \bar{u}_{m+1,n-1}^x) + F\bar{u}_{m,n}^y + G(\bar{u}_{m-1,n}^y + \bar{u}_{m+1,n}^y) = 0,$$

$$E = \frac{\tan(hk)}{2k}, \quad F = k(-1 + \cot(hk))^2 + \frac{1}{2 - 2hk \cot(hk)} \tan(hk),$$

$$H = \frac{k \tan(hk)}{-4 + 4hk \cot(hk)}, \quad G = \frac{k(2 \cot(hk) - 2hk \operatorname{cosec}(hk)^2 + \tan(hk))}{-4 + 4hk \cot(hk)}.$$

From the coefficients, we see that there is a singularity when  $h \cot(hk) = 1$ . This is why we observe in Figure 2 that for  $k = \pi(2n + 1)/2h$ ,  $n = 1, 2, \dots$ , the coefficients shoot up, leading to severe deterioration in the conditioning of the system matrix. The coefficients of the new NIM are

$$A = -\frac{(-1 + e^{ikh})^3}{2e^{ikh} - 4e^{2ikh} + 2e^{3ikh}(1 + h^2k^2)}, \quad D = \frac{-1 + e^{2ikh}(1 + e^{-ikh} - e^{ikh} - 2h^2k^2)}{2e^{ikh} - 4e^{2ikh} + 2e^{3ikh}(1 + h^2k^2)},$$

$$B = \frac{i(-1 + \frac{1}{2}(e^{-ikh} + e^{ikh}))hk}{-2 - \frac{1}{2}(e^{-ikh} - e^{ikh})h^2k^2 + \frac{1}{2}(e^{-ikh} + e^{ikh})(2 + h^2k^2)}, \quad E = \frac{(-1 + e^{ikh})h}{-1 + e^{ikh}(1 + i hk)}.$$

From these coefficients, we can see that for  $h \neq 0$  and real  $k$ , there is no singularity present any more, and thus the system matrix conditioning does not have sensitive dependence on the wave number  $k$  any more.

## References

1. Kumar N. and Gander M. J.: A new nodal integration method for Helmholtz problems based on domain decomposition techniques. *Proc. 27th Int. Conf. Domain Decomp. Methods.* **135**, 1–61 (2022)
2. Wu F: Discontinuous Galerkin Methods for the Helmholtz Equation with Large Wave Number. *SIAM J. Numer. anal.* **47**, 1–10 (2009)
3. Hiptmair R. and Moiola A. and Perugia I.: Trefftz discontinuous Galerkin methods for acoustic scattering on locally refined meshes. *Appl. Numer. Math.* **79**, 79–91 (2014)
4. Hiptmair R. and Moiola A. and Perugia I.: Plane wave discontinuous Galerkin methods for the 2D Helmholtz equation: Analysis of the p-version *SIAM J. Numer. Anal.* **49**, 264–284 (2011)
5. Rizwan-uddin: An Improved Coarse-Mesh Nodal Integral Method for Partial Differential Equations. *Numer. Methods Partial Differ. Equ.* **13**, 113–145, (1997)
6. Griesmaier R. and Monk P.: Error analysis for a hybridizable discontinuous Galerkin method for the Helmholtz equation. *SIAM J. Sci. Comput.* **40**, 291–310 (2011)
7. Kumar N. and Shekar B. and Singh S.: A nodal integral scheme for acoustic wavefield simulation. *Pure Appl. Geophys.* **179**, 3677–3691 (2022)
8. Després B.: Décomposition de domaine et problème de Helmholtz. *C.R. Acad. Sci. Paris.* **1**, 313–316 (1990)
9. Babuska, Ivo M. and Sauter, Stefan A.: Is the pollution effect of the FEM avoidable for the Helmholtz equation considering high wave numbers? *SIAM J. Numer. Anal.* **34**, 2392–2423 (1997)
10. Ernst, Oliver G. and Gander, Martin J.: Why it is difficult to solve Helmholtz problems with classical iterative methods. *Numer. Anal. Multiscale Probl.* **1**, 325–363 (2012)
11. Trefftz, Erich: Ein Gegenstück zum Ritzschen Verfahren. *Proc. 2nd Int. Cong. Appl. Mech. Zurich.* **1**, 131–137 (1926)
12. Walter R.: Über eine neue Methode zur Lösung gewisser Variationsprobleme der mathematischen Physik. *J. Reine Angew. Math.* **135**, 1–61 (1909)
13. Cocquet, P. H., Gander, M. J., Xiang X: Closed form dispersion corrections including a real shifted wavenumber for finite difference discretizations of 2d constant coefficient Helmholtz problems. *SIAM J. Sci. Comput.* **43**, A278–A308 (2021)